

In Silico Analysis of Natural Product-like Acetylcholinesterase Inhibitors and Rational Design of Novel High Affinity Ligands

ISCI 3A12 – Independent Project Final Paper

Eric Pettipiece

Dr. Jim McNulty

April 15, 2022

Abstract

Alzheimer's Disease (AD) is the most prevalent neurodegenerative disorder in the world, impacting over 44 million people globally. Decreased cerebral acetylcholine concentration is postulated to be a major factor responsible for the reduction of cognitive function in AD patients. Therefore, significant research has been dedicated to the development of acetylcholinesterase (AChE) inhibitors, resulting in the approval of drugs such as reminyl, rivastigmine and donepezil, although these drugs have recognized limited efficacy. One other promising class of compounds are the chalcones – natural products that can easily be synthesized and derivatized in the lab. This project examined the binding energy and docking pose of synthetic chalcones *in silico* using the programs AutoDock Vina and ChimeraX, with the aim of correlating predicted binding energy with experimentally determined IC₅₀ values. The X-Ray crystal structure of AChE was obtained online (PDB ID: 4EY7) and prepared for docking in AutoDock Vina. Ligand molecules were drawn in Chem3D, energy minimized, and docked with AChE in AutoDock Vina, while results were visualized in ChimeraX. Plotting the obtained binding energies against IC₅₀ values showed no correlation. Further QSAR analysis of the interaction between chalcones and AChE showed no correlation between electronic character of the benzene rings and binding energy but did identify the trifluoromethyl group as a significant element in the pharmacophore. Using this information two novel ligands, DAG and cTCO-Tz, were developed that exhibited -12.1 kcal/mol and -13.5 kcal/mol binding energy, respectively. It is anticipated that the number of people suffering from AD will continue to increase as the population ages, underscoring the importance for the identification of new lead compounds for drug discovery. Here, *in silico* molecular docking has provided two such compounds.

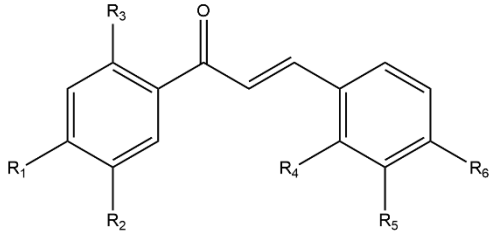
Introduction

Alzheimer's Disease (AD) is the most common cause of dementia globally.¹ The disease is characterized by an increase in amyloid- β plaques in the brain, neurofibrillary tangles, and a decrease in neuronal acetylcholine concentration.^{1,2} Disease progression is typically associated with loss of cognitive function, memory loss, and confusion – likely due to a combination of the aforementioned physiological changes.¹ Despite widespread efforts, the underlying causes of AD remain unknown and as such there are no approved cures for the disease and all currently marketed pharmaceuticals merely slow the progression of symptoms associated with AD.^{3–5} The most common mechanism employed by these drugs is the inhibition of the enzyme acetylcholinesterase (AChE), which is responsible for the hydrolysis of acetylcholine.⁶ One of the benefits of targeting AChE for the management of AD symptoms is that it is very well studied, with its overall structure and active site well defined.^{6–9} The enzyme is a globular serine hydrolase that catalyzes the hydrolysis of acetylcholine into acetic acid and choline, resulting in the termination of nerve signalling.⁶ Crystal structures of the enzyme are commonly reported as dimers, with each monomer being composed of 542 amino acid residues.^{7,10} The binding domain of AChE is a narrow gorge approximately 20 Å deep, with the catalytic triad of S234, H478, and E365 located at the bottom along with an oxyanion hole composed of W267, F326, and F328 that help to stabilize the tetrahedral intermediate during the breakdown of acetylcholine.^{7,11} The mouth of the active site gorge is ringed primarily by aromatic amino acids that compose the peripheral anionic binding site – a location that can be exploited in the design of inhibitor molecules by optimizing for π stacking interactions.¹² By inhibiting AChE, the resulting increase in neuronal acetylcholine concentration slows the cognitive decline typically associated with AD. There are three commonly prescribed small molecule AChE inhibitors for the treatment of AD: galantamine (Reminyl®), rivastigmine

(Exelon®), and donepezil (Aricept®) – all of which have realized limited efficacy.⁴ As such, there is a need for novel, potent, and accessible AChE inhibitors.

One class of compounds that are currently under investigation for their AChE inhibitory activity are the chalcones.^{13–15} Chalcones are abundant natural products that have demonstrated a wide array of biological activities, ranging from anti-inflammatory to anti-fungal.¹⁶ The scaffold for these compounds is a simple 1,3-diaryl-2-propene-1-one backbone, and the aryl rings can easily be functionalized by reagent selection to give compounds with varying polarity and electronic character.¹⁷ Another major benefit of chalcones is their ease of synthesis, with methods including a Claisen-Schmidt condensation between acetophenone and benzaldehyde, a palladium catalyzed Suzuki cross coupling of benzoyl chloride and phenylvinylboronic acid, Wittig olefination using triphenylphosphoniumbenzoylmethylene and benzaldehyde, or a Friedel-Crafts acylation of an aromatic ether and cinnamoyl chloride.¹⁷ It is also worth noting that chalcones can also be used as Michael acceptors in conjugate addition reactions as they possess an α - β unsaturated carbonyl in their structure, which allows for interesting functionalization of the aliphatic chain of the molecule.¹⁷ From an analytical perspective, chalcones are also easy to work with as they are fully conjugated and can thus be analyzed by UV-Vis spectroscopy, such as in the widely used Ellman assay.¹⁸ In this study, a small library of eight chalcones (Table 1), generated by a base-catalyzed Claisen-Schmidt condensation, was examined *in silico* to assess the binding interactions of these ligands with AChE.

Table 1: Library of synthetic chalcones examined in this study. The scaffold was generated using differentially substituted benzaldehyde and acetophenone reagents in a base catalyzed Claisen-Schmidt condensation. Prime designation denotes substitution on the acetophenone ring.

Chalcone Backbone	Name	ID
	2'-hydroxy-4-methoxychalcone	1a
	4'-hydroxy-3,4-dimethoxy-3'-methylchalcone	1b
	4'-hydroxy-4-methoxy-2-methylchalcone	1c
	4'-hydroxy-3'-methylchalcone	1d
	2'-hydroxy-2,4-dimethoxychalcone	1e
	4'-hydroxy-3,4-dimethoxychalcone	1f
	4'-hydroxy-4-methoxy-3'-methylchalcone	1g
	2'-hydroxy-3,4-dimethoxychalcone	1h

Computer-based molecular docking software has significantly improved the speed of initial hit identification using virtual screening (VS) of compound libraries.¹⁹ Both academic and industrial laboratories can make use of this powerful tool to narrow down the field of potentially active compounds to save time and resources during traditional *in vitro* high-throughput screening (HTS).²⁰ The basis of molecular docking studies is simple: the ligand molecule, either drawn by the researcher or extracted from an online compound library, is docked with the crystal structure of the target of interest such as an enzyme. In most docking studies, the ligand is a flexible molecule capable of adopting different conformations while the target is kept rigid.²¹ This greatly simplifies the docking simulation and saves computing power while still producing sufficiently accurate results. All molecular docking software use specific sampling methods and scoring functions to evaluate the conformational position of the ligand at a target site and its binding affinity, but different programs will use different suites of algorithms to sample and position ligand molecules in a target site. Some of the most common types of algorithms include matching, incremental construction, LUDI, molecular dynamics, and stochastic methods such as Monte Carlo or genetic algorithms.²¹ While the sampling function creates the various poses of the ligand

binding, the scoring function is what decides which conformations are “correct” or “incorrect” based on a calculation of various protein-ligand binding energies. Broadly, scoring functions are divided into three categories: force-field-based, empirical, and knowledge-based.²² In all cases, it is important to remember that scoring functions are optimized to provide sufficiently accurate results while maintaining high computational speed, and thus make assumptions and estimations during the calculation process.^{21,22} This study utilized the program AutoDock Vina to carry out all docking analysis.²³ AutoDock Vina demonstrates massive improvement in both computational speed and accuracy compared to previous versions of AutoDock by utilizing a new iterated local search global optimizer algorithm as well as an improved empirical scoring function (Equation 1).^{23–25}

$$\Delta G = W_{s1} \times \text{gauss}_1 + W_{s2} \times \text{gauss}_2 + W_R \times \text{Repulsion} + W_{hp} \times \text{Hydrophobic} + W_{hb} \times \text{HB} + W_{rot} N_{rot} \quad (1)$$

Where the first three terms of the scoring function are the steric interactions of the receptor and ligand, and the following are the terms for hydrophobic interactions, hydrogen bonding, and torsional strain of the ligand, respectively.

Molecular docking offers several benefits over traditional *in vitro* high throughput screening, primarily regarding speed and resource requirements. Using an *in silico* method for an initial screen of a library of compounds is significantly faster than any laboratory-based assay and does not involve any associated reagent costs. However, molecular docking is a model and an estimation of the binding affinity of a ligand to a receptor. Any result obtained from a docking procedure must be experimentally validated and thus molecular docking cannot be used as an isolated technique for the screening of compound libraries.^{26,27} Rather, it should be used as a pre-

screening technique that may help to reduce the number of compounds tested *in vitro* and improve the hit rate of experimental assays.²⁸ Molecular docking is also incredibly useful as a tool for rational drug design – a low throughput method of identifying lead compounds whereby novel molecules are developed based on knowledge of the 3D structures of the ligand and receptor as well as key interactions at the target site.^{28–30} This approach offers promising potential for drug discovery in light of the often disappointing results from high-throughput screening-based methods. Moreover, improvements in structural elucidation technologies such as X-ray crystallography and cryo-electron microscopy have allowed access to more accurate target structures that can be used for the design of novel compounds.²⁸ In this study, rational drug design was used to generate novel structures that exhibit promise as lead compounds for the inhibition of AChE.

Methods

Preparation of Receptor

The crystal structure of AChE was obtained online (PDB ID: 4EY7) and prepared for docking using MGLTools 1.5.7. The structure 4EY7 is a homodimer of AChE co-crystallized with donepezil in the binding site, which allowed for the easy identification of the docking region. Chain B of the structure was deleted along with all water molecules and other co-crystallized small molecules, leaving only chain A of the enzyme. Polar hydrogens were added to chain A, which was then checked for any missing atoms. Three instances of missing atoms were identified and repaired by the program, and then saved as two separate files. Kollman charges were then added to the enzyme, checked, and atom type was assigned before checking for any non-bonded atoms. The final prepared structure was then saved as an AutoDock PDBQT file for docking.

Ligand Preparation

All ligands in this study were prepared in Chem3D (PerkinElmer, USA) either by directly drawing the molecule (novel ligands) or using the name-to-structure function (chalcones and donepezil). All structures were energy minimized in Chem3D and double checked to ensure that a logical structure was produced. Instances where structures did not make sense, such as a meta-hydroxy group that was not hydrogen bonding to the carbonyl in the chalcones, were manually corrected and energy minimized again. Chem3D does not allow for structures to be saved directly as a PDBQT file, so structures were saved as an SDF file type and then converted to the required PDBQT format in OpenBabel 3.1.1.³¹

Docking Procedure and Parameters

Ligands were docked with AChE in AutoDock Vina using the default parameters. The centre of the grid box was located at (-13.514, -43.001, 26.985) and each side of the box was set to length 55. These dimensions were determined visually in ADT 1.5.7 using the co-crystallized donepezil as a reference. For each docking run a maximum of 10 outputs was allowed, with a maximum energy range between the best and worst result set to 4 kcal/mol.

Visualization of Results

All docking results were visualized in UCSF ChimeraX 1.3.³² Docking poses of each compound were checked for errors such as atom clashes through visual inspection and the result with the lowest binding energy was taken to be the best estimate of a compounds actual binding.

Validation of Docking

To validate the accuracy of the docking procedure a re-docking of donepezil into AChE was performed. Donepezil was drawn in Chem3D as previously specified and docked with AChE in AutoDock Vina using the same parameters as all other runs. The RMSD between the actual co-crystallized pose of donepezil and the re-docked pose was calculated in ChimeraX by importing PDB ID 4EY7 and the re-docked output into the same session and using the ‘rmsd’ command.

Determination of Binding Site Interactions

To better determine the binding interaction between the ligand molecules and AChE the Protein-Ligand Interaction Profiler (PLIP) web tool was used.³³ This tool takes a single PDB file as an input and provides information on the residues involved in hydrogen bonding, pi stacking, hydrophobic interactions, and other intermolecular forces between a ligand and a receptor. Since each docking result is its own PDBQT file, a series of protein-ligand complex PDB files had to be generated in ChimeraX. Each ligand docking result (10 ligand poses) was loaded separately into the prepared AChE PDBQT file and all poses besides the best were deleted. The resulting AChE-liagnd complex was then combined and saved as a single MOL2 file which was then converted to PDB format using OpenBabel 3.1.1. This PDB file was then used as the input for the PLIP web tool.

Pharmacokinetic Parameter Estimation

Pharmacokinetic parameters of the developed novel ligands were estimated using the online web tool SwissADME.³⁴ The chemical structures were drawn in Chem3D and converted to their SMILES strings, which were then used as the input for the SwissADME tool.

Statistical Analysis

All statistical analysis for the QSAR study was performed in Microsoft Excel using the data analysis extension. A two-way ANOVA was used to determine if there was any statistically significant difference in binding energy between substitution of the benzaldehyde or acetophenone ring and the electronic effect of different substituents. Significance value was set at $\alpha = 0.05$.

Results and Discussion

Chalcone Binding Analysis

Initial docking of the chalcones into the crystal structure of AChE was used to extract the predicted binding pose and binding energy of the interaction. Figure 1 is a representative example of the chalcone binding in the active site gorge of AChE.

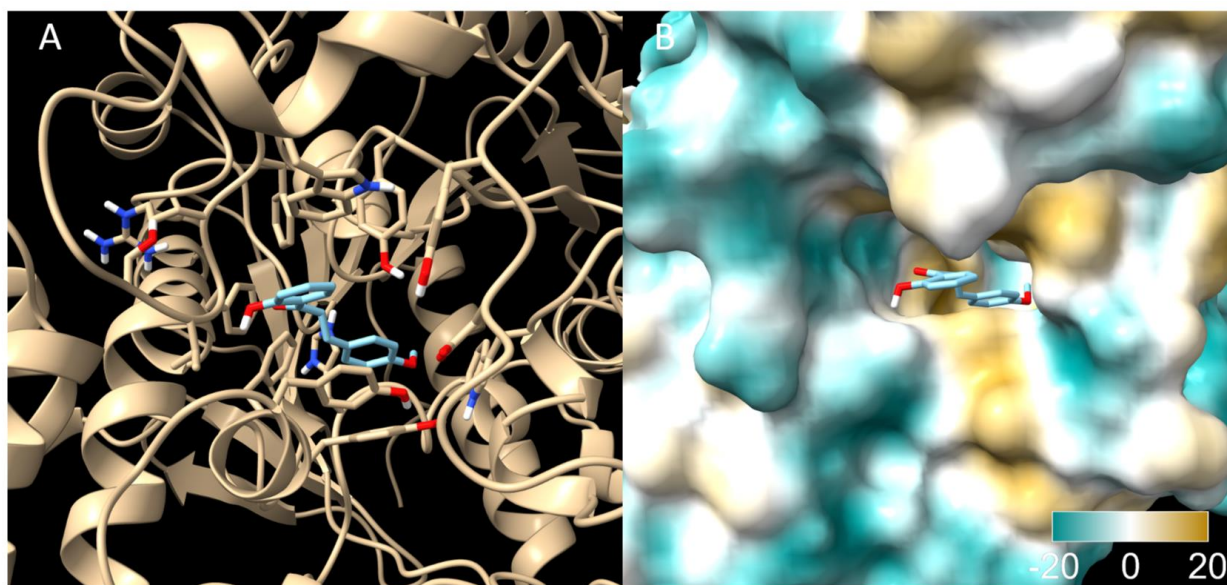
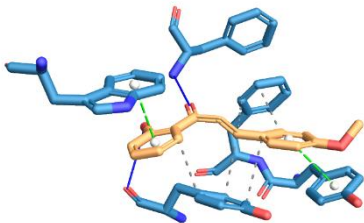
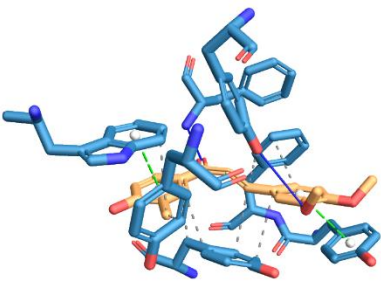
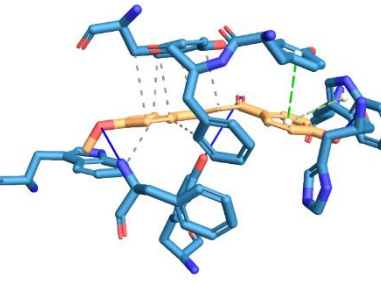
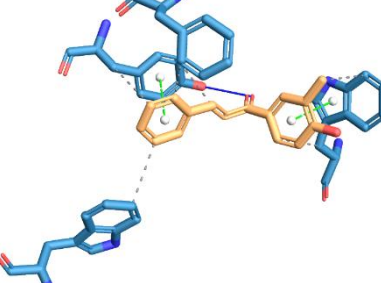
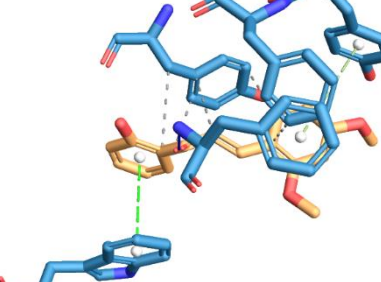


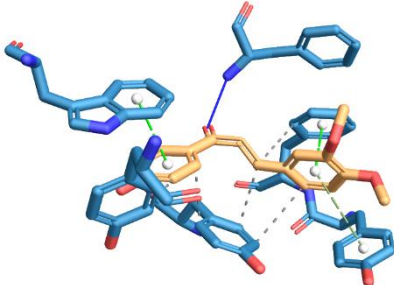
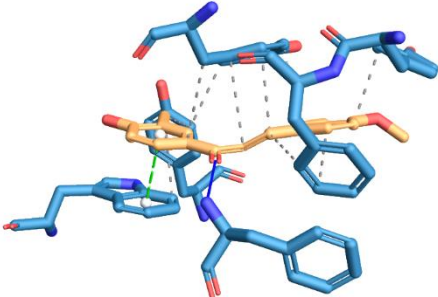
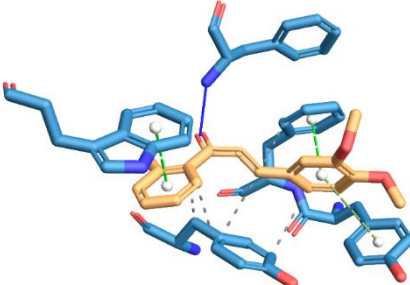
Figure 1: Representative binding example of a chalcone in the active site gorge of AChE. (A) Docking of the chalcone **1a** (blue) with the ribbon diagram of AChE (beige). Amino acid residues within a 5 Å radius of the chalcone have their side chains shown. (B) Hydrophobic surface representation of AChE clearly showing the active site gorge where the chalcone binds. Cyan colouring represents regions of low hydrophobicity and yellow represents high hydrophobicity. Images produced in UCSF ChimeraX.

In all cases the chalcones interacted exclusively with aromatic amino acid residues in the active site gorge of AChE, excluding ligand **1c** which also formed a single hydrogen bond to His 438. Interestingly, this hydrogen bond was formed between the 4' hydroxyl group of the chalcone and the backbone carbonyl of histidine. It is unknown as to why only this chalcone interacted with the histidine residue as five of the eight chalcones in the library contain a hydroxyl group on the 4' carbon. Since the His 438 residue is deeper in the active site gorge than all other interacting amino acids one hypothesis is that the differential substitution on the benzaldehyde aromatic ring restricts the depth to which the chalcone binds in the gorge, preventing the interaction. However, compound **1d** does not have any substituents on the benzaldehyde ring and does not interact with His 438, suggesting that this might not actually be the reason. The most important amino acid residues (i.e. interactions conserved in six or more of the chalcones) include Trp 277, Phe 286, Tyr 328, Phe 329, and Tyr 332, suggesting that the chalcones primarily interact with AChE through hydrophobic or Pi stacking interactions. The calculated binding energy of the chalcones ranged from -9.7 to -10.4 kcal/mol. All binding interactions are summarized in Table 2.

Table 2: Summary of chalcone binding interactions with AChE. Visualized binding interaction and specific amino acid interactions are taken from the Protein-Ligand Interaction Profiler. Chalcone is shown in orange and AChE residues are shown in blue. Bolded amino acids are conserved interactions across at least six of the eight chalcones. Binding energies are those calculated in AutoDock Vina.

ID	Binding Interaction	Interacting Amino Acids	Binding Energy (kcal/mol)
1a		<p>Hydrophobic Interaction (gray dash): Phe 329, Tyr 332</p> <p>Hydrogen bonds (blue solid): Phe 286, Tyr 332</p> <p>Pi stacking (green dash): Trp 277, Tyr 328</p>	-9.7

1b		<p>Hydrophobic interaction (gray dash): Tyr 69, Trp 277, Phe 329, Tyr 332</p> <p>Hydrogen bonds (blue solid): Tyr 121, Phe 286</p> <p>Pi stacking (green dash): Trp 277, Tyr 328</p>	-10.4
1c		<p>Hydrophobic interaction (gray dash): Trp 277, Phe 329, Tyr 332</p> <p>Hydrogen bonds (blue solid): Tyr 121, Phe 286, His 438</p> <p>Pi stacking (green dash): Trp 83, Tyr 328</p>	-10.3
1d		<p>Hydrophobic interaction (gray dash): Trp 86, Trp 277, Phe 329, Tyr 332</p> <p>Hydrogen bonds (blue solid): Tyr 332</p> <p>Pi stacking (green dash): Trp 86, Tyr 332</p>	-10.0
1e		<p>Hydrophobic interaction (gray dash): Phe 329, Tyr 332</p> <p>Hydrogen bonds (blue solid): Phe 286</p> <p>Pi stacking (green dash): Trp 277, Tyr 328</p>	-9.8

1f		<p>Hydrophobic interaction (gray dash): Tyr 69, Phe 329, Tyr 332</p> <p>Hydrogen bonds (blue solid): Phe 286</p> <p>Pi stacking (green dash): Trp 277, Tyr 328, Phe 329</p>	-9.9
1g		<p>Hydrophobic interaction (gray dash): Tyr 69, Trp 277, Tyr 328, Phe 329, Tyr 332</p> <p>Hydrogen bonds (blue solid): Phe 286</p> <p>Pi stacking (green dash): Trp 277</p>	-10.3
1h		<p>Hydrophobic interaction (gray dash): Phe 329, Tyr 332</p> <p>Hydrogen bonds (blue solid): Phe 286</p> <p>Pi stacking (green dash): Trp 277, Tyr 328, Phe 329</p>	-10.0

Comparing these interactions with those of re-docked donepezil shows that the residues important for chalcone binding are the same as those for the binding of donepezil to AChE, namely Trp 277, Phe 286, Phe 329, and Tyr 332. This provides extremely strong evidence for the importance of hydrophobic and pi stacking interactions for ligand binding at the active site gorge and highlights a key area for future ligand optimization.

The key residues involved in pi stacking with the chalcones were Trp 277 and Tyr 328, both of which have electron rich aromatic side chains. The chalcones docked in this study were also all electron rich, containing either methoxy, hydroxyl, or methyl groups on the aromatic rings. Therefore, a logical optimization of these ligands is to change their electronic character from electron rich to electron poor by changing their substituents. This in theory should increase the strength of the pi stack interactions and improve the overall binding affinity of the ligands. To test this hypothesis the compound **1a** had its hydroxyl and methoxy substituents removed and a trifluoromethyl group was added to the meta position of the acetophenone ring. This resulted in a decrease in binding energy (i.e. increase in binding affinity) from -9.7 kcal/mol to -11.1 kcal/mol (Figure 2). Addition of a second trifluoromethyl group on the benzaldehyde ring of the chalcone demonstrated a further decrease in binding energy to -11.5 kcal/mol.

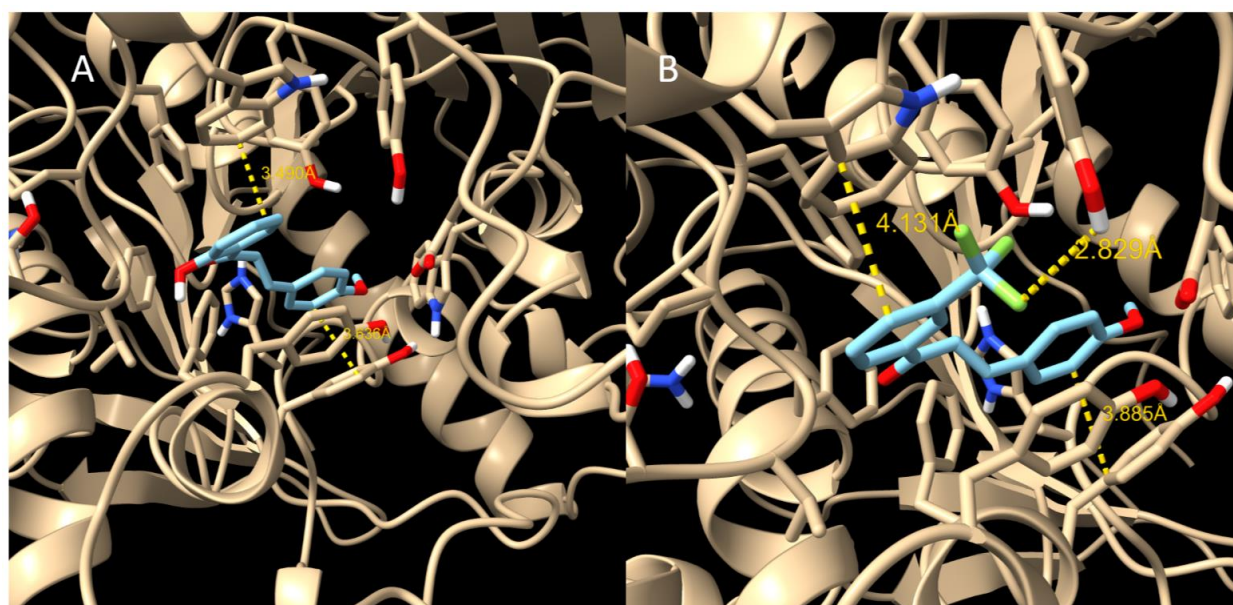


Figure 2: Optimization of the chalcone binding interaction. (A) Binding interaction between chalcone **1a** (blue) and AChE (beige) – binding energy for this interaction is -9.7 kcal/mol. Pi stacking interactions are shown as yellow dashes with the distance in angstroms. (B) Optimized chalcone where the electron donating substituents on the rings were removed and replaced by a trifluoromethyl group. Binding energy of this interaction is -11.1 kcal/mol and a new hydrogen bond between one of the fluorine atoms (green) and the hydroxyl group of Tyr 72. Images created in UCSF ChimeraX.

Excited by these results and wishing to explore the influence of ring electronic character on binding energy further, we conducted a quantitative structure activity relationship (QSAR) assay. In this experiment various electron donating groups (EDG) and electron withdrawing groups (EWG) were substituted onto the para position of either the acetophenone or benzaldehyde rings and the binding energy was plotted against the Hammett electronic parameter for each substituent. Table 3 summarizes the substituents used in this experiment, their Hammett parameters, and the calculated binding energies. The Hammett electronic parameter is a measure of the electron withdrawing or donating capacity of a functional group when substituted on an aromatic ring. It was derived by Louis Hammett in 1937 who noted the linear free-energy relationship between reaction rates and equilibrium constants of benzoic acid derivatives with meta and para substituents.³⁵ Since its introduction, the Hammett electronic parameter has been a useful tool for examining the impact of aromatic electronic character on binding interactions.³⁶

Table 3: Summary of QSAR study. Substituents were selected to give a wide range of electron donating and withdrawing capacities to better elucidate the role of ring electronics. The Hammett parameters used in this study are all for para substituted rings.

Substituent	Hammett Parameter	Binding Energy – Acetophenone Substituted (kcal/mol)	Binding Energy – Benzaldehyde Substituted (kcal/mol)
NMe ₂	-0.83	-10.1	-9.9
NH ₂	-0.66	-9.8	-9.8
OH	-0.37	-9.8	-9.8
OMe	-0.268	-9.8	-9.9
CH ₃	-0.17	-10.2	-10.1
H	0	-9.7	-9.7
F	0.062	-10.0	-9.9
Cl	0.227	-9.8	-10.0
COOEt	0.45	-10.1	-10.1
CF ₃	0.54	-10.9	-10.8
CN	0.66	-9.9	-9.8
NO ₂	0.778	-10.2	-10.3

It was hypothesized that if binding were solely influenced by the electronic character of the aromatic rings of the chalcone there would be a trend toward lower binding energy as the electron withdrawing capacity of the substituents increased. This was generally observed as shown in Figure 3a, which plots the binding energy of the best scoring docking pose against the Hammett parameter. However, there was no significant difference between the mean binding energy of any of the substituents by ANOVA ($p > 0.05$). Furthermore, there was no statistically significant difference ($p > 0.05$) in mean binding energy when comparing the same substituent on either the acetophenone or benzaldehyde ring using a two-sample t-test assuming equal variance (Figure 3b). Despite there being no statistically significant difference between the mean binding energy of any of the substituents, there was an evident increase in binding affinity of the best scoring pose when the trifluoromethyl group was used as the substituent on the rings. This suggests that the trifluoromethyl group may be an important element in the pharmacophore of the AChE binding site and thus was used in the later development of a novel ligand.

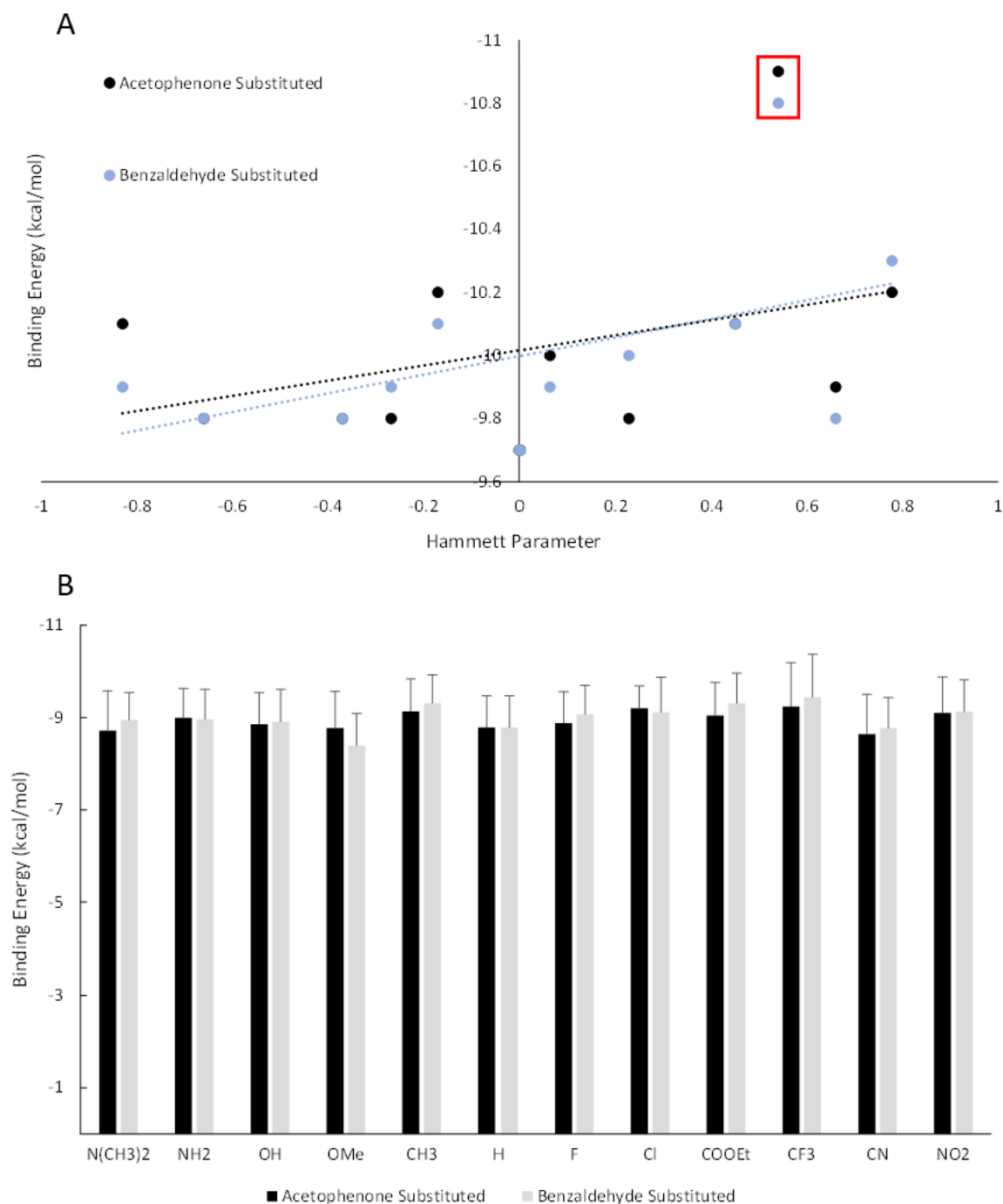


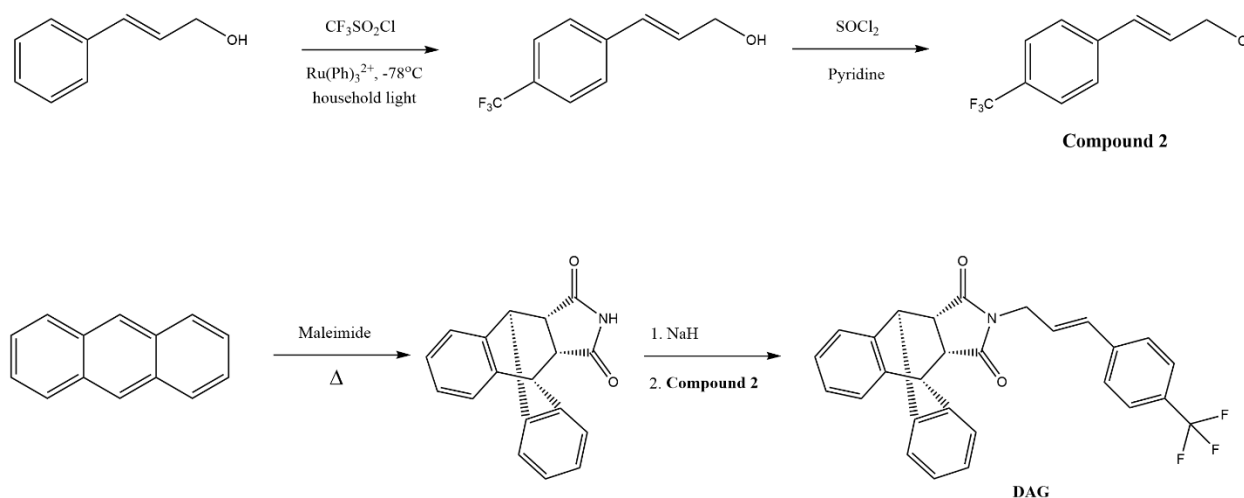
Figure 3: Quantitative structure activity relationship analysis. (A) Plot of the best binding poses of the differentially substituted chalcones examined in the QSAR experiment against the Hammett para electronic parameter of the substituents tested. There is a slight trend towards better binding as the electron withdrawing capacity of the substituent increases. The trifluoromethyl binding energy was an outlier and is boxed in red. (B) Comparison of the mean binding energy ($n = 10$) of the differentially substituted chalcones examined in the QSAR analysis. No significant difference was observed between substituents, or between which ring the substitution was on.

To further examine the binding interaction between chalcones and AChE the carbonyl group of compound **1a** was removed and the new structure redocked into the enzyme. The calculated binding energy of the new structure was determined to be -9.6 kcal/mol – only 0.1 kcal/mol different than compound **1a**. Intrigued by this result, three other structures were generated; one structure replaced the carbonyl group with an amine, another with CH₂, and the final structure was the 4'-trifluoromethyl substituted chalcone from the QSAR analysis without its carbonyl group. The amine and CH₂ substituted compounds showed better binding than compound **1a** at -10.1 kcal/mol each, while the 4'-trifluoromethyl compound demonstrated still superior binding with a calculated energy of -10.5 kcal/mol – 0.4 kcal/mol worse binding than the carbonyl-containing compound. These results suggest that the carbonyl group of the chalcones is not necessary for their binding to AChE and the primary mode of interaction is likely through hydrophobic and pi stacking interactions as well as the interactions from the trifluoromethyl group. Moreover, the removal of the carbonyl group removes the reactive Michael acceptor in the chalcone, thereby reducing its potential to react with nucleophilic species. While this does not directly impact *in silico* studies, the lack of a reactive centre in the molecule may be of critical importance for future *in vivo* studies where external interferences are abundant.

Design of Novel Ligands for the Inhibition of AChE

Based on the results of the chalcone binding analysis above, two novel ligands were rationally designed to bind the active site of AChE. Both ligands demonstrated excellent binding energy, exceeding that of re-docked donepezil (-11.5 kcal/mol) which was used as the baseline reference for “good” binding. The first of the two ligands, (9R,10S,11R,15S)-13-((E)-3-(4-(trifluoromethyl)phenyl)allyl)-9,10-dihydro-9,10-[3,4]epipyrroloanthracene-12,14-dione, herein

referred to as **DAG** (**Diels-Adler Gabriel** after the important synthetic steps) was inspired by the chalcone binding interaction. As such, a para trifluoromethyl group was installed on cinnamyl alcohol using triflyl chloride and a ruthenium photocatalyst³⁷ which was then converted to *p*-trifluoromethyl cinnamyl chloride using thionyl chloride. Since the mouth of the active site gorge of AChE is ringed by aromatic amino acids and is quite narrow, it was thought that the replacement of the acetophenone ring with a more sterically bulky aromatic moiety would act as an “anchor” for the molecule. This was achieved through a Diels-Alder cycloaddition between anthracene and maleimide, which was then coupled to the derivatized cinnamyl chloride using a Gabriel-like synthesis without the hydrolysis step. Scheme 1 shows the proposed synthetic strategy for the formation of **DAG**.



Scheme 1: Proposed synthetic scheme for novel ligand **DAG**. Initial reaction of cinnamyl alcohol with triflyl chloride using a photocatalyst results in the para substituted trifluoromethyl group. The alcohol is then converted to an alkyl chloride using thionyl chloride under basic conditions. Generation of the bulky “anchor” is a one step Diels-Alder cycloaddition between anthracene and maleimide. The final product is produced using a Gabriel-like synthesis.

Docking of ligand **DAG** into the crystal structure of AChE resulted in a binding energy of -12.1 kcal/mol and a binding pose that was nearly exactly as intended during the design of the

molecule, with the anthracene-maleimide Diels-Alder adduct getting “stuck” on the mouth of the gorge and the *p*-trifluoromethyl cinnamyl moiety binding within the gorge itself (Figure 4).

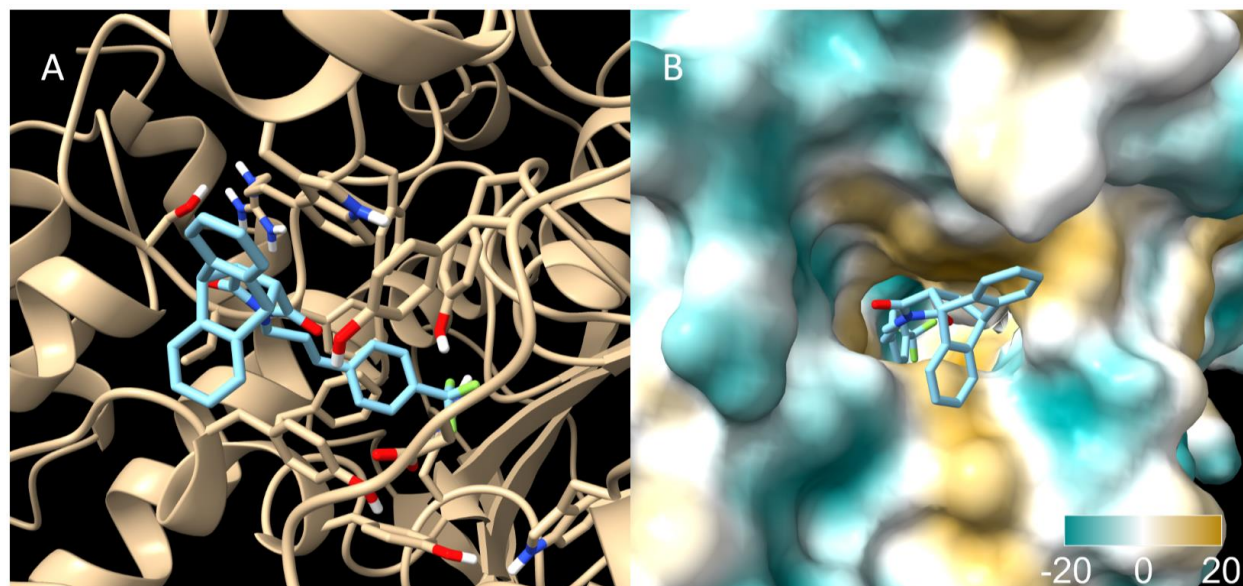


Figure 4: Binding pose of novel ligand **DAG**. (A) Binding interaction between **DAG** (blue) and the ribbon diagram of AChE (beige), resulting in a calculated binding energy of -12.1 kcal/mol. Amino acids within a 5 Å radius of **DAG** have their side chains shown. (B) Hydrophobic surface representation of the binding between **DAG** and AChE. Note that the ligand binds as predicted, with the bulky anthracene moiety getting “stuck” at the mouth of the active site gorge while the rest of the molecule binds in a similar manner to the chalcones. Cyan colour represents regions of low hydrophobicity and yellow represents regions of high hydrophobicity. Images generated in UCSF ChimeraX.

The second ligand designed in this study, (E)-1-(2-methoxyphenyl)-3-(3,5,14,14a-tetrahydridibenzo[4,5:6,7]cycloocta[1,2-d]pyridazin-8-yl)prop-2-en-1-one, herein referred to as **cTCO-Tz** (chalcone **trans**-cyclooctene-**t**etrazine), is another chalcone-inspired molecule with a sterically bulky multi-cyclic ring system replacing one of the benzene rings. Originally, only the biphenyl *trans*-cyclooctene tetrazine ligation product was designed as the novel ligand as it was predicted to bind at the mouth of the active site gorge due to its high bulk and aromatic rings. However, docking this molecule into the crystal structure of AChE revealed that it bound further down in the active site gorge than even the chalcones (Figure 5a). Overlaying the docking pose of

compound **1a** with this new ligand showed overlap between the benzaldehyde aromatic ring of the chalcone and one of the benzene rings of the cyclooctene derivative (Figure 5b). Therefore, the two molecules were combined into **cTCO-Tz** and redocked (Figure 5c/d), resulting in an outstanding binding energy of -13.5 kcal/mol.

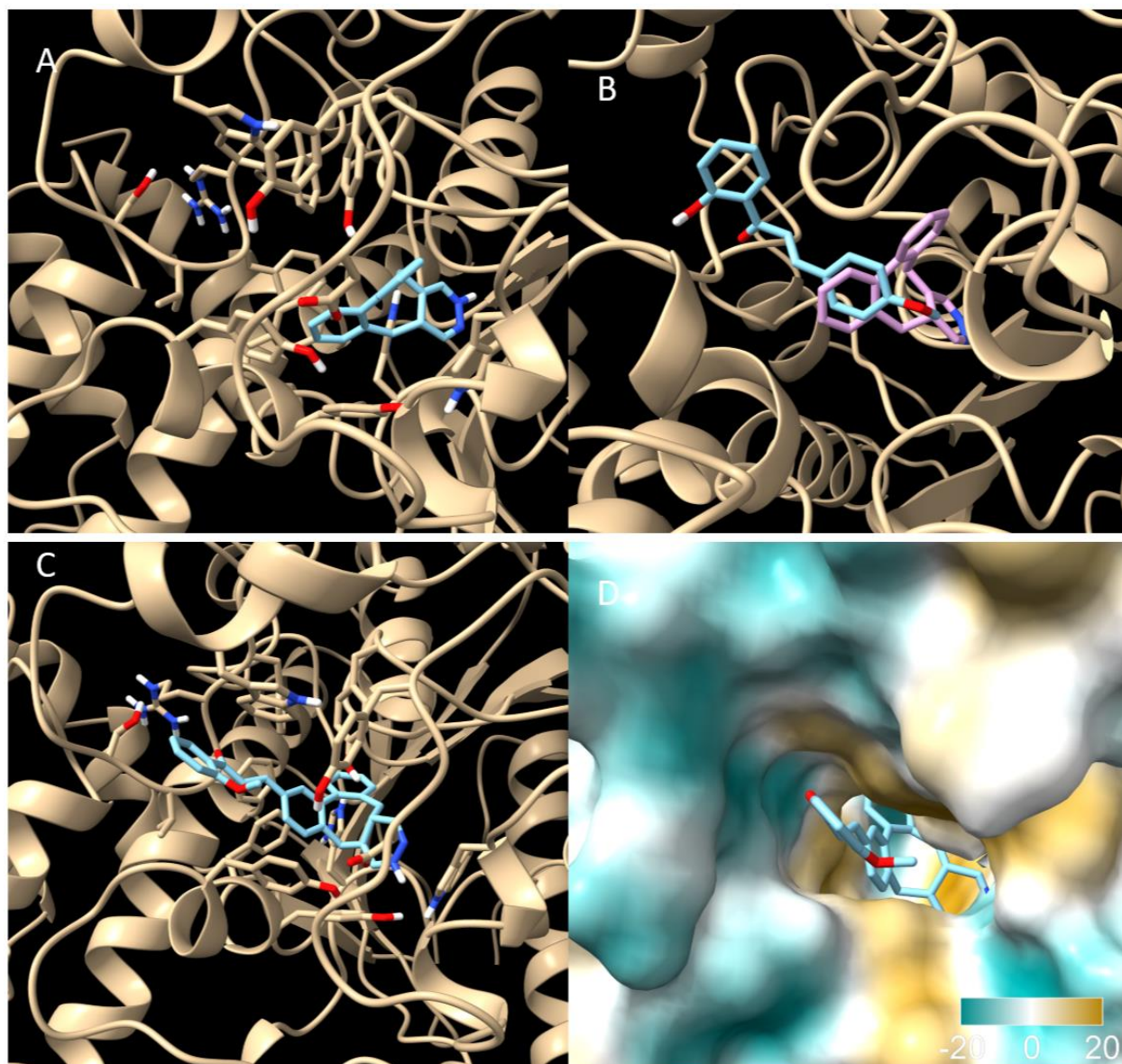
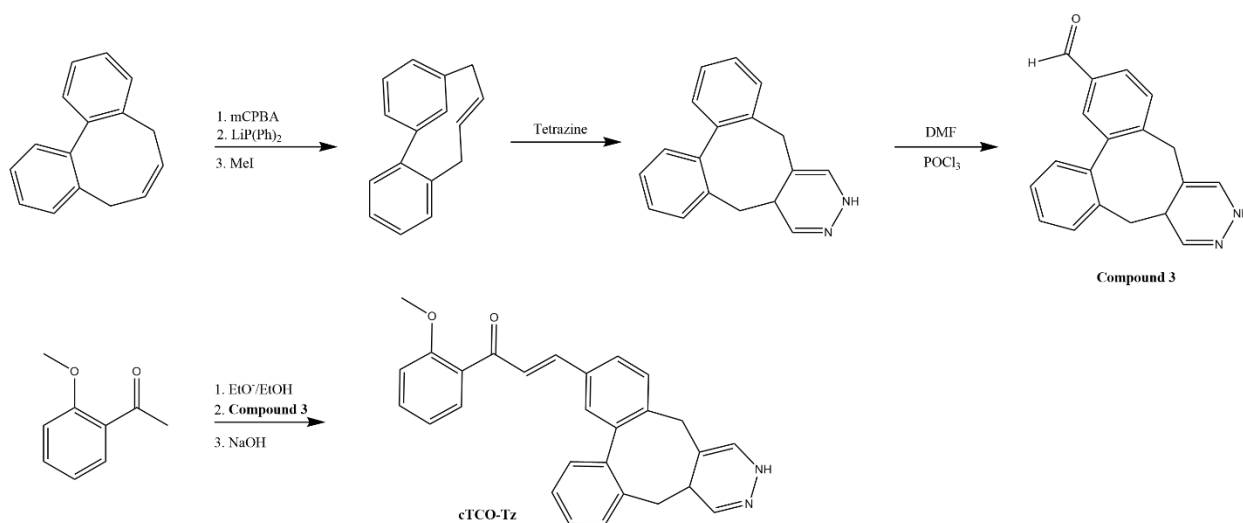


Figure 5: Binding interaction between **cTCO-Tz** and AChE. (A) Binding of the biphenyl cyclooctene ligand (blue) originally designed for the inhibition of AChE (beige). Note that this ligand binds further down in the active site gorge than the chalcones examined in this study. (B) Overlap of the aromatic rings of the chalcone **1a** and the biphenyl cyclooctene ligand which prompted the combination of these moieties. (C) Best binding pose of the novel ligand **cTCO-Tz**

(blue) docked into the active site gorge of AChE (beige). Amino acid residues within a 5 Å radius of **cTCO-Tz** have their side chains shown. This interaction had an excellent binding energy of -13.5 kcal/mol. (D) Hydrophobic surface model highlighting the excellent fit of the novel ligand **cTCO-Tz** within the active site gorge of AChE. Cyan colours represent regions of low hydrophobicity and yellow regions represent areas of high hydrophobicity. Images created in UCSF ChimeraX.

The synthesis of **cTCO-Tz** requires (Z)-5,8-dihydrodibenzo[a,c][8]annulene to be isomerized into the *E* configuration in order to carry out the trans-cyclooctene tetrazine ligation step.³⁸ This isomerization can be achieved first by epoxidating the alkene followed by epoxide opening with lithium diphenyl phosphide and methylation using methyl iodide.³⁹ This reaction proceeds through a betaine intermediate and generates the isomerized ring in high yield and stereoselectivity.³⁹ Alternatively, photoisomerization is another method that has recently been used to isomerize cyclooctene derivatives and may be applicable to the synthesis of this compound.⁴⁰ Following isomerization and ligation with tetrazine, a formyl group is introduced onto one of the aromatic rings via the Vilsmeier-Haack formylation.⁴¹ This product is then reacted with 2-methoxyacetophenone in a base-catalyzed Claisen-Schmidt condensation to generate the final product (Scheme 2).

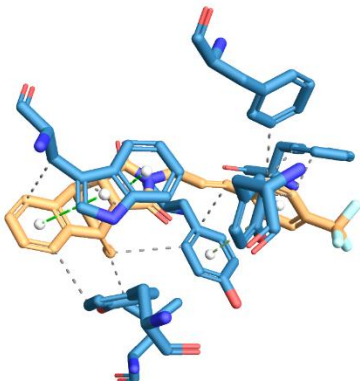
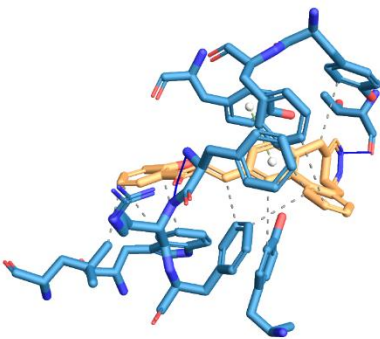


Scheme 2: Synthetic scheme for the novel ligand **cTCO-Tz**. Initial starting material can be special ordered from Sigma-Aldrich. Isomerization of the cyclooctene ring is accomplished through

epoxide opening using diphenylphosphide followed by methylation. The strained trans product is then reacted with tetrazine to form the originally designed ligand. Formylation of the benzene ring is accomplished using the Vilsmeier-Haack formylation and this intermediate is then used in a base-catalyzed Claisen-Schmidt condensation to generate the final product.

Like the chalcone binding analysis, the specific interactions between the novel ligands and AChE were assessed in the Protein-Ligand Interaction Profiler. Unsurprisingly, the novel ligands interacted with all the residues that were conserved between the chalcones, including Trp 277, Phe 286, Tyr 328, Phe 329, and Tyr 332. This was expected as the structures of the novel ligands were inspired by the chalcones. Table 4 summarizes the complete interaction between the ligands and AChE.

Table 4: Summary of the binding interactions between the novel ligands **DAG** and **cTCO-Tz** and AChE. Ligands are shown in orange and the amino acid residues of AChE are shown in blue. Bolded amino acids are those which were previously identified as conserved interactions for chalcone binding. Binding energy was calculated in AutoDock Vina.

Ligand	Binding Interaction	Interacting Amino Acids	Binding Energy (kcal/mol)
DAG		Hydrophobic interactions (gray dash): Tyr 69, Leu 73, Tyr 121, Trp 277 , Phe 288, Phe 329 , Tyr 332 Hydrogen bonds (blue solid): N/A Pi stacking (green dash): Trp 277 , Tyr 332	-12.1
cTCO-Tz		Hydrophobic interactions (gray dash): Tyr 121, Trp 277 , Leu 280, Phe 288, Tyr 328 , Phe 329 Hydrogen bonds (blue solid): Thr 80, Phe 286 , Arg 287 Pi stacking (green dash): Tyr 332	-13.5

One of the main limitations of molecular docking is that the binding grid is specifically defined by the user, essentially forcing the ligands into the known active site of whatever target is being examined. As such, it is possible that ligands may bind better to other areas of the target when tested *in vitro* or *in vivo*. To get a sense for ligand selectivity for the active site of AChE a blind docking run was conducted. Blind docking is a process in which the grid box is set to its maximum size to encapsulate the entire enzyme, allowing ligands to bind anywhere and not just the region of interest. If ligands continue to bind at the active site of the enzyme, it is possible that they may be potent inhibitors and worth further investigation. From the blind docking study, it was noted that **DAG** bound in the active site for two of the three top poses (-9.3 and -9.0 kcal/mol) but primarily bound a different site of AChE (Figure 6a). The ligand **cTCO-Tz** bound the active site of AChE with most of the poses (Figure 6b), including its five best with binding energies ranging from -8.6 to -9.3 kcal/mol.

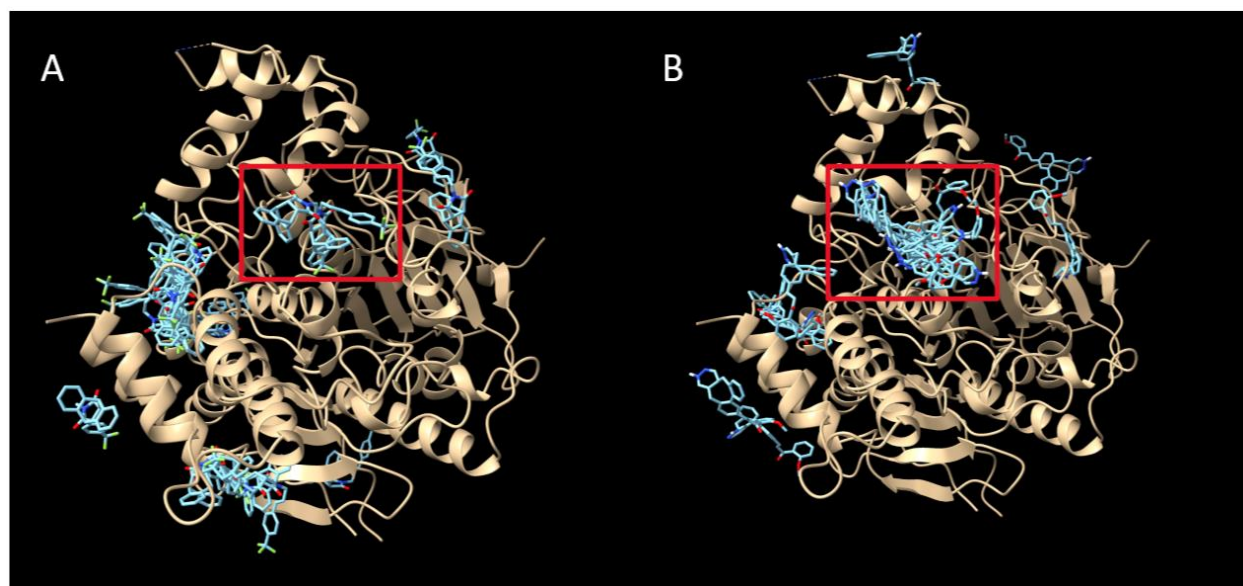


Figure 6: Blind docking of the novel ligands **DAG** and **cTCO-Tz**. (A) Blind docking analysis of the novel ligand **DAG** which showed that only two of the 20 docked poses bound at the active site of AChE (red box). However, these two poses were the best and third best ranked by binding energy. (B) Blind docking analysis of the novel ligand **cTCO-Tz** which showed that the ligand

primarily bound at or around the active site of AChE (red box). The top five best docked poses were all found in this region. Images created in UCSF ChimeraX.

Thus far, this study has focused on the pharmacodynamics of the chalcones and novel ligands. While this is important and helps to establish whether these molecules interact properly with AChE there is much more to an effective drug. Of course, a drug cannot enact its effect without getting to its target. A detailed pharmacokinetic study of these compounds is outside the scope of this project, but through utilizing web-based pharmacokinetic predictors, such as SwissADME, a predicted pharmacokinetic profile of the compounds may be generated. Indeed, both **DAG** and **cTCO-Tz** were analyzed using the SwissADME service which predicted neither compound to be completely drug-like based on various rule sets such as Lipinski's rule of 5, Ghose's lead-likeness, and others.³⁴ Additionally, **DAG** was predicted to not cross the blood-brain barrier (BBB) which is a considerable issue given that its target is in the brain. This problem could be solved by modifying the overall polarity of the compound by adding or removing functional groups without compromising binding energy. Ligand **cTCO-Tz** is predicted to cross the BBB and requires minimal optimization, with the primary concern being the presence of a reactive Michael acceptor in the molecule. Overall, the novel ligands created here require minimal to moderate pharmacokinetic optimization based on their predicted properties. It will not be until *in vivo* studies are conducted that we will know the true kinetics of these compounds.

Limitations of the Docking Study

Despite promising results from the *in silico* analysis of the chalcones and novel ligands, there are limitations to this type of study. First, it is important to note that all results reported in this paper *must* still be experimentally validated prior to drawing any conclusions about their potential as lead compounds for new AD treatments. In fact, using data generated from the

CHEMBIO 2L03 lab course for the chalcones studied in this project there is poor linearity between the binding energy calculated in AutoDock Vina and the IC_{50} values of the chalcones (Figure 7). This may be due in part to the low quality of the data obtained from the lab course and also the sub-par accuracy of the docking model, which was calculated to be 4.226 Å by the method previously described. This is below the typical accuracy threshold of 2 Å used in most molecular docking studies, suggesting that there is room for improvement in the docking model.

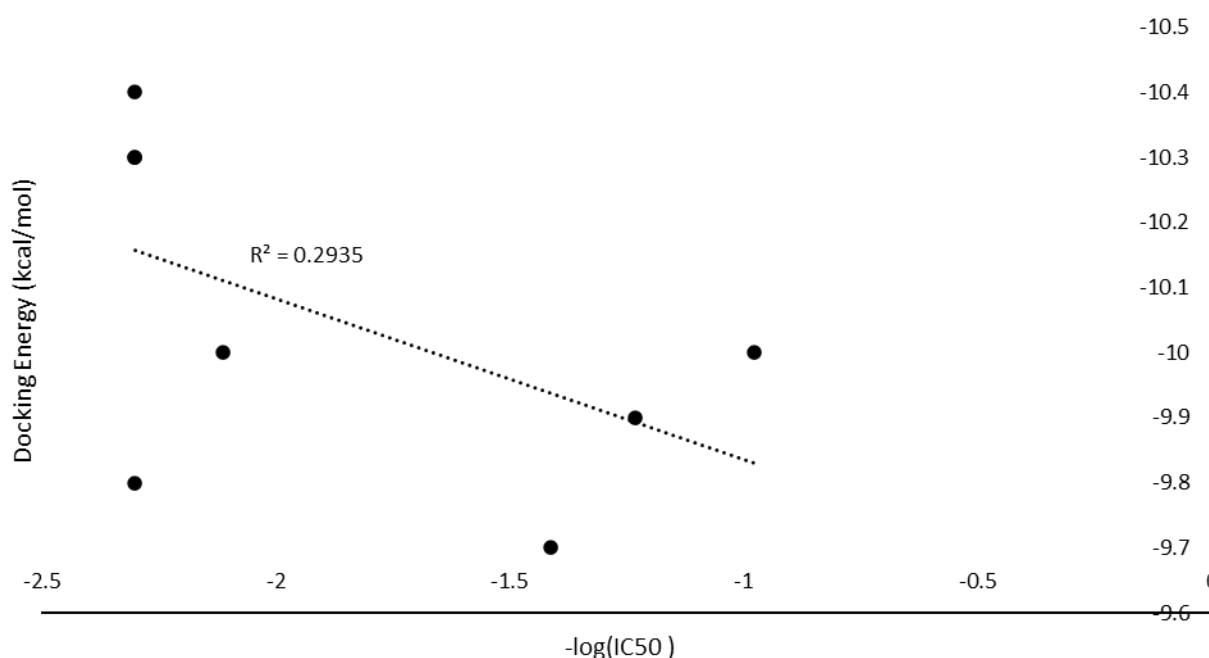


Figure 7: Relationship between calculated binding energies in AutoDock Vina and experimentally determined IC_{50} values of the chalcones studied. IC_{50} values were determined using the Ellman assay and any values > 100 mM were not specifically reported. For the purposes of this study these values were arbitrarily set at 200 mM. The resulting linearity between the calculated binding energies in AutoDock Vina and the experimental data is poor – highlighting the importance of validating docking results with high quality experimental data.

Conclusion

The incidence of Alzheimer's Disease is predicted to increase as the world's population ages, meaning there is more need than ever for efficacious and novel treatments.¹ Here, *in silico* molecular docking has demonstrated its potential in assisting in the development of these new lead compounds. Analysis of natural product-like chalcones helped to elucidate the important interactions within the enzyme active site gorge and establish a relationship between the electronic character of ligand aromatic rings and predicted binding energies. These interactions and trends culminated in the creation of two novel ligands that demonstrated higher affinity for the enzyme than all currently marketed treatments for AD. These novel ligands are synthetically accessible and require only minimal to moderate pharmacokinetic optimization based on predicted "drug-likeness" scores and blood brain barrier penetration. Future work will be directed towards the synthesis of these compounds to establish optimal synthetic conditions and determine their efficacy *in vitro* to demonstrate if they are in fact potent inhibitors of AChE. The results of this study indicate that rational drug design and creative organic chemists are still a relevant and useful tool in drug discovery and should be considered in compliment to traditional high throughput techniques.

References

- (1) Tiwari, S.; Atluri, V.; Kaushik, A.; Yndart, A.; Nair, M. Alzheimer's Disease: Pathogenesis, Diagnostics, and Therapeutics. *Int. J. Nanomedicine* **2019**, *14*, 5541–5554. <https://doi.org/10.2147/IJN.S200490>.
- (2) Francis, P. T. The Interplay of Neurotransmitters in Alzheimer's Disease. *CNS Spectr.* **2005**, *10* (S18), 6–9. <https://doi.org/10.1017/S1092852900014164>.
- (3) Yiannopoulou, K. G.; Papageorgiou, S. G. Current and Future Treatments in Alzheimer Disease: An Update. *J. Cent. Nerv. Syst. Dis.* **2020**, *12*, 1179573520907397. <https://doi.org/10.1177/1179573520907397>.
- (4) Marucci, G.; Buccioni, M.; Ben, D. D.; Lambertucci, C.; Volpini, R.; Amenta, F. Efficacy of Acetylcholinesterase Inhibitors in Alzheimer's Disease. *Neuropharmacology* **2021**, *190*, 108352. <https://doi.org/10.1016/j.neuropharm.2020.108352>.
- (5) McHardy, S. F.; Wang, H.-Y. L.; McCowen, S. V.; Valdez, M. C. Recent Advances in Acetylcholinesterase Inhibitors and Reactivators: An Update on the Patent Literature (2012-2015). *Expert Opin. Ther. Pat.* **2017**, *27* (4), 455–476. <https://doi.org/10.1080/13543776.2017.1272571>.
- (6) Dvir, H.; Silman, I.; Harel, M.; Rosenberry, T. L.; Sussman, J. L. Acetylcholinesterase: From 3D Structure to Function. *Chem. Biol. Interact.* **2010**, *187* (1–3), 10–22. <https://doi.org/10.1016/j.cbi.2010.01.042>.
- (7) Cheung, J.; Rudolph, M. J.; Burshteyn, F.; Cassidy, M. S.; Gary, E. N.; Love, J.; Franklin, M. C.; Height, J. J. Structures of Human Acetylcholinesterase in Complex with Pharmacologically Important Ligands. *J. Med. Chem.* **2012**, *55* (22), 10282–10286. <https://doi.org/10.1021/jm300871x>.
- (8) Silman, I.; Sussman, J. L. Acetylcholinesterase: How Is Structure Related to Function? *Chem. Biol. Interact.* **2008**, *175* (1), 3–10. <https://doi.org/10.1016/j.cbi.2008.05.035>.
- (9) Kryger, G.; Harel, M.; Giles, K.; Toker, L.; Velan, B.; Lazar, A.; Kronman, C.; Barak, D.; Ariel, N.; Shafferman, A.; Silman, I.; Sussman, J. L. Structures of Recombinant Native and E202Q Mutant Human Acetylcholinesterase Complexed with the Snake-Venom Toxin Fasciculin-II. *Acta Crystallogr. D Biol. Crystallogr.* **2000**, *56* (11), 1385–1394. <https://doi.org/10.1107/S0907444900010659>.
- (10) Franklin, M. C.; Rudolph, M. J.; Ginter, C.; Cassidy, M. S.; Cheung, J. Structures of Paraoxon-Inhibited Human Acetylcholinesterase Reveal Perturbations of the Acyl Loop and the Dimer Interface. *Proteins Struct. Funct. Bioinforma.* **2016**, *84* (9), 1246–1256. <https://doi.org/10.1002/prot.25073>.
- (11) Silva, M. A.; Kiametis, A. S.; Treptow, W. Donepezil Inhibits Acetylcholinesterase via Multiple Binding Modes at Room Temperature. *J. Chem. Inf. Model.* **2020**, *60* (7), 3463–3471. <https://doi.org/10.1021/acs.jcim.9b01073>.
- (12) Agatonovic-Kustrin, S.; Kettle, C.; Morton, D. W. A Molecular Approach in Drug Development for Alzheimer's Disease. *Biomed. Pharmacother.* **2018**, *106*, 553–565. <https://doi.org/10.1016/j.biopha.2018.06.147>.
- (13) Liu, H.; Liu, X.; Fan, H.; Tang, J.; Gao, X.; Liu, W.-K. Design, Synthesis and Pharmacological Evaluation of Chalcone Derivatives as Acetylcholinesterase Inhibitors. *Bioorg. Med. Chem.* **2014**, *22* (21), 6124–6133. <https://doi.org/10.1016/j.bmc.2014.08.033>.
- (14) Zhao, F.-C.; Wu, Y.; Song, X.-J. Design and Development of a Novel Chalcone Derivative as an Anticholinesterase Inhibitor for Possible Treatment of Dementia. *Med. Sci. Monit. Int. Med. J. Exp. Clin. Res.* **2017**, *23*, 3311. <https://doi.org/10.12659/MSM.901842>.
- (15) Díaz-Rubio, L.; Hernández-Martínez, R.; Estolano-Cobián, A.; Chávez-Velasco, D.; Salazar-Aranda, R.; Waksman de Torres, N.; Rivero, I. A.; García-González, V.; Ramos, M. A.; Córdova-Guerrero, I. Synthesis, Biological Evaluation and Docking Studies of Chalcone and Flavone Analogs as Antioxidants and Acetylcholinesterase Inhibitors. *Appl. Sci.* **2019**, *9* (3), 410. <https://doi.org/10.3390/app9030410>.

- (16) Salehi, B.; Quispe, C.; Chamkhi, I.; El Omari, N.; Balahbib, A.; Sharifi-Rad, J.; Bouyahya, A.; Akram, M.; Iqbal, M.; Docea, A. O.; Caruntu, C.; Leyva-Gómez, G.; Dey, A.; Martorell, M.; Calina, D.; López, V.; Les, F. Pharmacological Properties of Chalcones: A Review of Preclinical Including Molecular Mechanisms and Clinical Evidence. *Front. Pharmacol.* **2021**, *11*, 592654. <https://doi.org/10.3389/fphar.2020.592654>.
- (17) Zhuang, C.; Zhang, W.; Sheng, C.; Zhang, W.; Xing, C.; Miao, Z. Chalcone: A Privileged Structure in Medicinal Chemistry. *Chem. Rev.* **2017**, *117* (12), 7762–7810. <https://doi.org/10.1021/acs.chemrev.7b00020>.
- (18) Ellman, G. L.; Courtney, K. D.; Andres, V.; Featherstone, R. M. A New and Rapid Colorimetric Determination of Acetylcholinesterase Activity. *Biochem. Pharmacol.* **1961**, *7* (2), 88–95. [https://doi.org/10.1016/0006-2952\(61\)90145-9](https://doi.org/10.1016/0006-2952(61)90145-9).
- (19) Maia, E. H. B.; Assis, L. C.; de Oliveira, T. A.; da Silva, A. M.; Taranto, A. G. Structure-Based Virtual Screening: From Classical to Artificial Intelligence. *Front. Chem.* **2020**, *8*.
- (20) Hughes, J. P.; Rees, S.; Kalindjian, S. B.; Philpott, K. L. Principles of Early Drug Discovery. *Br. J. Pharmacol.* **2011**, *162* (6), 1239. <https://doi.org/10.1111/j.1476-5381.2010.01127.x>.
- (21) Meng, X.-Y.; Zhang, H.-X.; Mezei, M.; Cui, M. Molecular Docking: A Powerful Approach for Structure-Based Drug Discovery. *Curr. Comput. Aided Drug Des.* **2011**, *7* (2), 146.
- (22) Huang, S.-Y.; Grinter, S. Z.; Zou, X. Scoring Functions and Their Evaluation Methods for Protein–Ligand Docking: Recent Advances and Future Directions. *Phys. Chem. Chem. Phys.* **2010**, *12* (40), 12899–12908. <https://doi.org/10.1039/C0CP00151A>.
- (23) Trott, O.; Olson, A. J. AutoDock Vina: Improving the Speed and Accuracy of Docking with a New Scoring Function, Efficient Optimization, and Multithreading. *J. Comput. Chem.* **2010**, *31* (2), 455–461. <https://doi.org/10.1002/jcc.21334>.
- (24) Huang, S.-Y. Comprehensive Assessment of Flexible-Ligand Docking Algorithms: Current Effectiveness and Challenges. *Brief. Bioinform.* **2018**, *19* (5), 982–994. <https://doi.org/10.1093/bib/bbx030>.
- (25) Eberhardt, J.; Santos-Martins, D.; Tillack, A. F.; Forli, S. AutoDock Vina 1.2.0: New Docking Methods, Expanded Force Field, and Python Bindings. *J. Chem. Inf. Model.* **2021**, *61* (8), 3891–3898. <https://doi.org/10.1021/acs.jcim.1c00203>.
- (26) Pinzi, L.; Rastelli, G. Molecular Docking: Shifting Paradigms in Drug Discovery. *Int. J. Mol. Sci.* **2019**, *20* (18), 4331. <https://doi.org/10.3390/ijms20184331>.
- (27) Llanos, M. A.; Gantner, M. E.; Rodriguez, S.; Alberca, L. N.; Bellera, C. L.; Talevi, A.; Gavernet, L. Strengths and Weaknesses of Docking Simulations in the SARS-CoV-2 Era: The Main Protease (Mpro) Case Study. *J. Chem. Inf. Model.* **2021**, *61* (8), 3758–3770. <https://doi.org/10.1021/acs.jcim.1c00404>.
- (28) Zhang, B.; Li, H.; Yu, K.; Jin, Z. Molecular Docking-Based Computational Platform for High-Throughput Virtual Screening. *CCF Trans. High Perform. Comput.* **2022**, *4* (1), 63–74. <https://doi.org/10.1007/s42514-021-00086-5>.
- (29) Lounnas, V.; Ritschel, T.; Kelder, J.; McGuire, R.; Bywater, R. P.; Foloppe, N. Current Progress in Structure-Based Rational Drug Design Marks a New Mindset in Drug Discovery. *Comput. Struct. Biotechnol. J.* **2013**, *5*, e201302011. <https://doi.org/10.5936/csbj.201302011>.
- (30) Anukanon, S.; Pongpamorn, P.; Tiyaibhorn, W.; Chatwichien, J.; Niwetmarin, W.; Sessions, R. B.; Ruchirawat, S.; Thasana, N. In Silico-Guided Rational Drug Design and Semi-Synthesis of C(2)-Functionalized Huperzine A Derivatives as Acetylcholinesterase Inhibitors. *ACS Omega* **2021**, *6* (30), 19924–19939. <https://doi.org/10.1021/acsomega.1c02875>.
- (31) O’Boyle, N. M.; Banck, M.; James, C. A.; Morley, C.; Vandermeersch, T.; Hutchison, G. R. Open Babel: An Open Chemical Toolbox. *J. Cheminformatics* **2011**, *3* (1), 33. <https://doi.org/10.1186/1758-2946-3-33>.
- (32) Pettersen, E. F.; Goddard, T. D.; Huang, C. C.; Meng, E. C.; Couch, G. S.; Croll, T. I.; Morris, J. H.; Ferrin, T. E. UCSF ChimeraX: Structure Visualization for Researchers, Educators, and Developers. *Protein Sci. Publ. Protein Soc.* **2021**, *30* (1), 70–82. <https://doi.org/10.1002/pro.3943>.

- (33) Adasme, M. F.; Linnemann, K. L.; Bolz, S. N.; Kaiser, F.; Salentin, S.; Haupt, V. J.; Schroeder, M. PLIP 2021: Expanding the Scope of the Protein–Ligand Interaction Profiler to DNA and RNA. *Nucleic Acids Res.* **2021**, *49* (W1), W530–W534. <https://doi.org/10.1093/nar/gkab294>.
- (34) Daina, A.; Michielin, O.; Zoete, V. SwissADME: A Free Web Tool to Evaluate Pharmacokinetics, Drug-Likeness and Medicinal Chemistry Friendliness of Small Molecules. *Sci. Rep.* **2017**, *7* (1), 42717. <https://doi.org/10.1038/srep42717>.
- (35) Hammett, L. P. The Effect of Structure upon the Reactions of Organic Compounds. Benzene Derivatives. *J. Am. Chem. Soc.* **1937**, *59* (1), 96–103. <https://doi.org/10.1021/ja01280a022>.
- (36) McKenzie, N.; McNulty, J.; McLeod, D.; McFadden, M.; Balachandran, N. Synthesizing Novel Anthraquinone Natural Product-like Compounds To Investigate Protein–Ligand Interactions in Both an in Vitro and in Vivo Assay: An Integrated Research-Based Third-Year Chemical Biology Laboratory Course. *J. Chem. Educ.* **2012**, *89* (6), 743–749. <https://doi.org/10.1021/ed200417d>.
- (37) Nagib, D. A.; MacMillan, D. W. C. Trifluoromethylation of Arenes and Heteroarenes by Means of Photoredox Catalysis. *Nature* **2011**, *480* (7376), 224–228. <https://doi.org/10.1038/nature10647>.
- (38) Johann, K.; Svatunek, D.; Seidl, C.; Rizzelli, S.; Bauer, T. A.; Braun, L.; Koynov, K.; Mikula, H.; Barz, M. Tetrazine- and Trans-Cyclooctene-Functionalised Polypept(o)ides for Fast Bioorthogonal Tetrazine Ligation. *Polym. Chem.* **2020**, *11* (27), 4396–4407. <https://doi.org/10.1039/D0PY00375A>.
- (39) Vedejs, E.; Snoble, K. A. J.; Fuchs, P. L. Phosphorus Betaines Derived from Cycloheptene and Cyclooctene Oxides. Inversion of Cyclooctene. *J. Org. Chem.* **1973**, *38* (6), 1178–1183. <https://doi.org/10.1021/jo00946a024>.
- (40) Shahbazali, E.; Billaud, E. M. F.; Fard, A. S.; Meuldijk, J.; Bormans, G.; Noel, T.; Hessel, V. Photo Isomerization of Cis-Cyclooctene to Trans-Cyclooctene: Integration of a Micro-Flow Reactor and Separation by Specific Adsorption. *AIChE J.* **2021**, *67* (1), e17067. <https://doi.org/10.1002/aic.17067>.
- (41) Meth-Cohn, O.; Stanforth, S. P. 3.5 - The Vilsmeier–Haack Reaction. In *Comprehensive Organic Synthesis*; Trost, B. M., Fleming, I., Eds.; Pergamon: Oxford, 1991; pp 777–794. <https://doi.org/10.1016/B978-0-08-052349-1.00049-4>.

Supplementary Data

DAG SMILES String:

O=C(N1C/C=C/C2=CC=C(C(F)(F)F)C=C2)[C@@H]3[C@@H]4C5=C([C@H]([C@@H]3C1=O)C6=C4C=CC=C6)C=CC=C5

cTCO-Tz SMILES String:

O=C(C1=C(OC)C=CC=C1)/C=C/C2=CC(C3=CC=CC=C3CC4C5=CCN=C4)=C(C5)C=C2

SwissADME web tool: <http://www.swissadme.ch/>

Protein-Ligand Interaction Profiler web tool: <https://plip-tool.biotec.tu-dresden.de/plip-web/plip/index>

Data availability: <https://github.com/pettipie/AChE-Docking-Files>